Toward Improving the Detection Rate of Gravitational Waves from Coalescing Binary Black Holes with Precessing Spin in LIGO/Virgo Data

Sara Frederick,[1] Stephen Privitera,[2,3] and Alan Weinstein[2,4]

[1] *Department of Physics & Astronomy, University of Rochester, Rochester, NY 14627*
[2] *LIGO Laboratory, California Institute of Technology, Pasadena, CA 91125*
[3] *Max Planck Institute for Gravitational Physics (Albert Einstein Institute), D-14476 Potsdam-Golm, Germany*
[4] *Department of Physics, Mathematics, and Astronomy, California Institute of Technology, Pasadena, CA 91125*

(Dated: January 19, 2015)

The Advanced LIGO and Virgo gravitational wave detectors will come online this year and are expected to outperform the strain sensitivity of initial LIGO/Virgo detectors by an order of magnitude and operate with greater bandwidth, possibly to frequencies as low as 10 Hz. Coalescing binary black holes (BBH) are anticipated to be among the most likely sources of gravitational radiation observable by the detectors. Searches for such systems benefit greatly from the use of accurate predictions for the gravitational wave signal to filter the data. The component black holes of these systems are predicted to have substantial spin, which greatly influences the gravitational waveforms from these sources; however, recent LIGO/Virgo searches have made use of banks of waveform models which neglect the effects of the component spins. The inclusion of spin effects in template waveforms is relatively simplified when the spins are aligned with the orbital angular momentum, since in that case the orientation of the binary orbital plane remains fixed. Although suboptimal, such filters are still sensitive to precessing signals. In this work, we quantify the expected improvement in signal-to-noise recovery by an aligned-spin template bank relative to a non-spinning template bank towards signals from generically precessing binary black holes. We also demonstrate how close such an aligned-spin template bank comes to being optimal in terms of signal-to-noise recovery. These results motivate our future development of a search pipeline implementing aligned spin template filters. We eventually aim to assess the ability of the `GSTLAL` gravitational wave search pipeline using IMR aligned-spin template waveforms to recover signals from generically spinning black hole binaries injected into simulated Advanced LIGO and Virgo detector noise. Currently, the search is limited only by the optimality of the template banks employed. Therefore we characterize the regions of the spin parameter space where template banks of given waveform models are effectual. If black holes are highly spinning as predicted, use of aligned-spin template banks in upcoming searches could increase the detection rate of these systems by as much as 170% for binaries with $\chi = 0.7$ spin in Advanced LIGO and Virgo data, compared to the previously non-spinning template banks.

Keywords: gravitational radiation, LIGO, Virgo, binary black hole mergers, black hole spin

I. INTRODUCTION

Gravitational waves are ripples in the fabric of space-time predicted by General Relativity (GR). According to GR, any dynamic, non-spherical gravitating system will radiate gravitational waves[1]. Taylor and Hulse, with their observation of pulsar binary PSR B1913+16 and its steadily decaying orbit, provided evidence of consistency with GR[2]. Since then, the theory has been verified by studying the orbital decay of other similar systems (some relativistic) and comparing these to the predicted amount of gravitational radiation lost[3].

Direct detection of gravitational waves is expected to usher in an entirely new era of observation. When a gravitational wave passes through space, it causes a local distortion of space-time. Strain is the fractional change in the measured distance between two freely-falling test masses due to the passage of gravitational waves. According to GR, a gravitational wave may be either cross- or plus-polarized (Figure 1). Gravitational wave signals are currently searched for by the LIGO Scientific Collaboration (LSC), which obtains data from two detectors in the United States —one in Hanford, WA and the other in Livingston, LA[4]. Other members of the worldwide gravitational wave observatory network are the Virgo Collaboration, which collects data from the Virgo gravitational wave antenna in Cascina, Italy, and the GEO Collaboration, which operates an interferometer near Hannover, Germany[5,6]. The detectors are composed of two identical perpendicular arms and measure gravitational wave strain via Michelson interferometry.

Detectable gravitational waves are produced by extreme and rapidly changing gravitational fields. Such conditions exist during events such as supernovae, and neutron star and/or black holes binary coalescences. Coalescing binary black holes (BBH) are the focus of this work. According to GR, binary combinations of black holes and neutron stars emit gravitational radiation which decreases their orbits. Given enough time, these binaries inspiral, then coalesce into a single black hole. When this occurs, the type of gravitational wave signal produced is described as a "chirp", due to its increasing frequency and amplitude. An example of a chirp waveform is shown in Figure 2. These compact binary

coalescences (CBCs) are prime targets for LIGO.

The formation of a compact binary is thought to follow from one of two origins. The first begins with a binary of main-sequence OB stars, which evolve together into compact binaries. The binary must outlast various mass exchanges, potentially including a common envelope stage, and two explosions as each component goes supernova, before arriving at the desired pair of compact objects. The second type evolves from a three-body system in which the outer third body shepherds the other two components into a close binary orbit. Knowledge of these processes are due in part to various population syntheses and numerical simulations of these systems. Evidence for the existence of these systems comes primarily from x-ray observations of black holes accreting matter from a companion star, and from radio observations of binary pulsars[7].

The way in which these compact binaries form is expected to produce components with large spin. The first compact binary evolution process described above may lead to component spins which are aligned with the orbital angular momentum of the system, due to the in-plane nature of the mass exchange processes[9]. If the supernova process gives a significant velocity or "kick" to the black hole during the binary formation, one or both of the components' spins may become misaligned with the system's orbital angular momentum. When both the component spin vectors and the orbital angular momentum precess about the total angular momentum axis, the orbital plane of the binary exhibits precession.

Any gravitational radiation compact binary mergers emit is extremely weak by the time they reach Earth. We employ a matched filter search to suppress instrumental background. The search relies on a matched-filter template bank —a collection of gravitational waveforms covering the relevant component mass and spin parameter space. Accurate waveform models are crucial to this method, which is why neglecting to account for the spin and precession of orbits may have consequences in the search for BBHs. Template bank generation serves as a preliminary part of the overall pipeline search.

The goal of this work is to implement an aligned-spin template bank in the `GSTLAL` search pipeline, and to assess the ability of these templates to capture both precessing and non-precessing (i.e. aligned-spin) signals. We look to maximize sensitivity to these signals for a given false alarm rate (FAR), without a decrease in the rate of detections recovered from the search pipeline. Typically non-spinning templates have been utilized, though sensitivity has been shown to improve with the use of spinning templates[10]. In this work, we look to take orbital precession into account with similar results. Previous studies have included aligned-spin effects into the injected signals, but were not able to make use of an IMR waveform model including precession[9,10]. Recently developed waveform models provide exactly this opportunity[11,12].

We will assess the sensitivity of the `GSTLAL` search pipeline to signals with and without precessing spin and for various templates at a fixed false alarm rate (FAR), described in Section **??**.

II. BACKGROUND

A. The Laser Interferometer Gravitational-wave Observatories

Gravitational wave signals are currently searched for by the LIGO Scientific Collaboration (LSC), which obtains data from two detectors in the United States —one in Hanford, WA and the other in Livingston, LA[4]. Other members of the worldwide gravitational wave observatory network are the Virgo Collaboration, which collects data from the Virgo gravitational wave antenna in Cascina, Italy, and the GEO Collaboration, which operates an interferometer near Hannover, Germany[5,6]. The detectors are composed of two identical perpendicular arms and measure gravitational wave strain via Michelson interferometry.

The strain of the gravitational wave signal $h = \frac{\Delta L}{L}$ is projected into the detector in the following way:

$$h = F_+(\theta, \phi, \psi)h_+ + F_\times(\theta, \phi, \psi)h_\times \tag{1}$$

where F_+ and $F_\times$ are the detector response functions to the two different gravitational wave polarizations and are defined as

$$F_+ = \frac{1}{2}(1+\cos(\theta)^2)\cos(2\phi)\cos(2\psi) - \cos(\theta)\sin(2\phi)\sin(2\psi) \tag{2}$$

and

$$F_\times = \frac{1}{2}(1+\cos(\theta)^2)\cos(2\phi)\sin(2\psi) - \cos(\theta)\sin(2\phi)\cos(2\psi). \tag{3}$$

Note that it is not trivial to perform this projection in the precessing case. For now, we merely follow what has been done in the aligned-spin case[9,21].

B. Status of Advanced LIGO

III. METHODS

A. Matched Filtering

The strain resulting from gravitational waves which reach Earth from compact binary sources is expected to be very weak ($\sim 10^{-21}$) compared to detector noise. Furthermore, LIGO observations are taken continuously over many years. Therefore, a computationally efficient method is needed to sift through the data for triggers, or potential signals. This method is the matched filter method, which correlates detector output with a template waveform, or a discrete set of waveforms in a template bank[13]. A matched filter template is a waveform

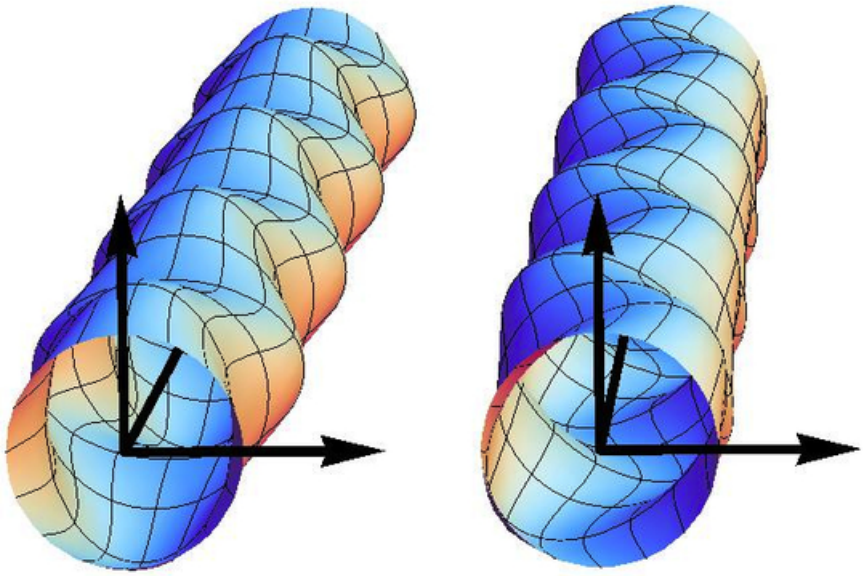

FIG. 1. The effect of plus-polarized (left) and cross-polarized (right) gravitational waves. The axis transverse to the ellipses can be viewed as time at a fixed location, or the third spatial dimension at a chosen time. The strain, depicted as the eccentricity of the ellipses, has been exaggerated for illustration.[9].

which, when it exactly matches the true signal, results in a maximal signal-to-noise ratio (SNR). In order for the SNR to be the optimal detection statistic, a stationary, Gaussian background must be assumed, although in reality the background is non-stationary and non-Gaussian. Therefore, many constraints are used in order to better treat the noise in the detector data (for example, the data are partitioned into segments which are approximately stationary over time).

The overlap of two signals is an inner product of the strain data $s(f)$ and the signal $h(f)$, divided by the PSD of the detector noise, $S_n(f)$:

$$\langle s,h\rangle = 2\int_{f_{low}}^{\infty} \frac{\tilde{s}(f)\tilde{h}^*(f)+\tilde{s}^*(f)\tilde{h}(f)}{S_n(f)}\,\mathrm{d}f. \qquad (4)$$

The signal-to-noise ratio time-series is defined as:

$$\rho(t) = \langle s,\hat{h}e^{2\pi i f t}\rangle = 4\int_{f_{low}}^{\infty} \frac{\tilde{s}^*(f)\hat{h}(f)}{S_n(f)}e^{2\pi i f t}\,\mathrm{d}f \qquad (5)$$

where $\hat{h}$ is h normalized as

$$\hat{h} = \frac{h}{\sqrt{\langle h|h\rangle}} \qquad (6)$$

and $\rho(t)$ is maximized over time. The match between a signal and a template is given by $\mathcal{M} = max\langle\hat{s},\hat{h}\rangle$, where the maximum is taken over all extrinsic parameters, and the mismatch is $1-\mathcal{M}$. We require a minimum match of $\mathcal{M} = 0.97$. The fitting factor of a signal taken over all the templates in a given bank is $FF = max(\mathcal{M})$. The detection volumes for the template bank V_{bank} and the optimal case V_{opt} at fixed SNR is related to the fitting factor in the following way:

$$FF^3 = \frac{V_{bank}}{V_{opt}}. \qquad (7)$$

Estimated increase in detection rate is then given by

$$\frac{V_{opt}}{V_{bank}} = \frac{1}{FF^3}. \qquad (8)$$

B. Waveform Models

Construction of banks of matched filters for the `GSTLAL` search requires accurate gravitational waveforms. We make use of the most recent of the family of phenomenological IMR waveforms, IMRPhenomP, which is similar to past models but includes precessing spin effects. These waveforms are created using both Post-Newtonian (for the inspiral) and Numerical Relativistic (for the merger and ringdown stages) prescriptions. The other family of IMR waveforms primarily used is EOBNR, or Effective One Body Numerical Relativity, waveforms[17,18]. SEOBNR, the waveform model which included component spins, now attempts to incorporate the effects of precessing spin in its third version[19]. Though we look to use IMRPhenomP for bank construction (restricted to aligned spin) and simulated injections, future work includes similar studies of the SEOBNR waveform model.

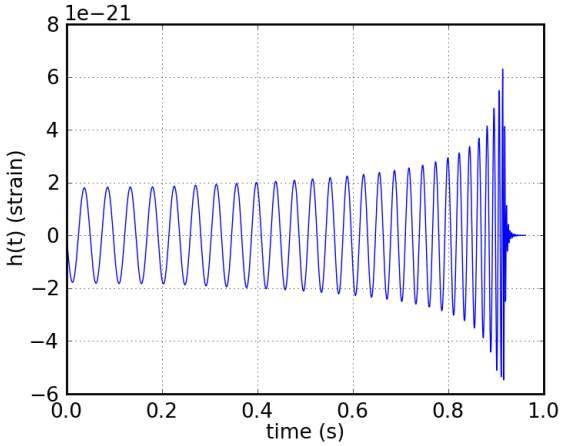

(a)IMR Waveform

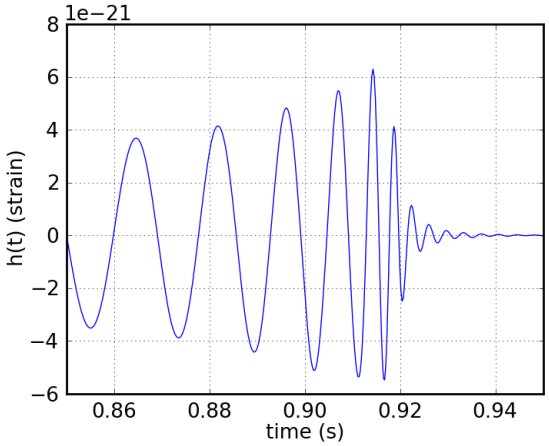

(b)Merger and Ringdown

FIG. 2. *Example of an inspiral-merger-ringdown (IMR) PhenomB waveform in the time domain. The chirp occurs in the growth of both strain amplitude and frequency of the inspiral phase and the sharp increase in both when the binary black hole merger occurs. The decay immediately following is the ringdown phase, where physical abnormalities in the shape of the resultant black hole are smoothed out via gravitational radiation. The waveform shown is for component masses of 20 and 40 solar masses ($M_\odot$) and no spin.*

θ, ϕ, and ψ (the polar, azimuth, and polarization angles, respectively) are the angles describing the source's location and orientation in the sky relative to a given detector. These observer-dependent parameters merely affect the amplitude of the signal strain. In the construction of a waveform, the other extrinsic parameters are inclination, coalescence time, coalescence phase, and distance (Table I). The intrinsic parameters, from which the waveform is fully determined apart from its amplitude, are component masses m_1 and m_2, and the components of each spin vector $\vec{s_1}$ and $\vec{s_2}$.

GR places an upper limit on the dimensionless spin parameter

$$\chi \equiv \frac{c}{G}\frac{S}{M^2} \tag{9}$$

of $\chi = 1$, and the black hole binaries observable by LIGO may have spins which are close to this maximum. Such features are evident in the signal from the gravitational radiation these sources emit. Positively-aligned-spin systems produce longer duration gravitational wave signals than non-spinning systems, whereas negatively-aligned-spin systems produce shorter duration waveforms than both[9]. Precession of the orbital plane is observable in the gravitational wave signal associated with the system as periodic modulation of the strain amplitude, as well as phase evolution of the strain signal[10].

In the non-precessing case, the spins of the component black holes may be resolved to a single parameter approximation χ_{eff}, such that

$$\chi_{eff} \equiv \frac{m_1 s_{1z} + m_2 s_{2z}}{m_1 + m_2} \tag{10}$$

in order to simplify parameter estimation[16]. We use only the z-components of the spins, since both spins are assumed to be aligned with the orbital plane.

Similarly, in the IMRPhenomP waveform model, $\chi_p(m_1, m_2, \vec{s_1}, \vec{s_2})$ is an effective parameter which approximately captures precession:

$$\chi_p \equiv \frac{S_p}{m_2^2} \tag{11}$$

where

$$S_p = \frac{max(A_1 S_{1\perp}, A_2 S_{2\perp})}{A_1} \tag{12}$$

such that $S_{i\perp}$ is the component of the i^{th} object's spin in the orbital plane and

$$A_i = 2 + \frac{3m_{3-i}}{2m_i} \tag{13}$$

assuming that m_2 is the mass of the larger black hole.[11]

C. Template Bank Construction

Researchers have continually improved the availability of binary black hole waveforms. We make use of analytic models which exhibit the appropriate phenomenology of the sources and verify them alongside numerical relativistic and post-Newtonian predictions. Use of aligned-spin template waveforms could increase detection rates of precessing and non-precessing signals in the upcoming Advanced LIGO observations. Parameters which are used to build the aligned-spin waveform include mass and spin of each black hole in the binary, plus many extrinsic parameters: right ascension, declination, inclination angle, polarization angle, coalescence time, coalescence phase, and

distance (Table I). Changing these parameters visibly affects the waveform in both the time and frequency domains (See Figure 3), although the extrinsic parameters only affect the strain's overall amplitude. Conversely, we can retrieve the masses and spins of a source from the waveform which most closely matches its signal.

right ascension	α
declination	δ
inclination angle	ι
polarization angle	ψ
coalescence time	t_{coal}
coalescence phase	ϕ_{coal}
distance	D

TABLE I. Extrinsic parameters used to construct gravitational waveforms. Extrinsic parameters depend only on the observer. Intrinsic parameters (not shown) consist of the component black holes' masses, m_1, m_2, and spins: s_{1x}, s_{2x}, s_{1y}, s_{2y}, s_{1z}, s_{2z}.

In order to cover the range of possible intrinsic parameters, we must construct discrete banks of templates with different values of those intrinsic parameters. We filter the data through all of the templates in the bank, and recover the parameter values from the templates which most closely fit the data. The parameter that quantifies the match between the template and the signal is the fitting factor (see Section **??**). In previous searches with inspiral-only, non-spinning templates, the banks were constructed using a lattice-based technique in which the templates were placed according to a parameter-space metric. Since no such metric exists for IMR waveforms, we make use of a stochastic algorithm for the construction of template banks. The template bank is arranged such that the templates are so close together in the parameter space that a signal will inevitably be similar enough to match it, to a level at or above a minimum match, which is usually taken to be 97%. Signals are simulated and injected into the bank to test their detection consistency with the aligned-spin templates. If we recover more injected signals than previous studies with non-spinning templates and/or non-precessing injections, this will indicate that this technique should be effective at increasing detection efficiency for future observations.

Many waveform models have been developed which incorporate additional physical features of candidate gravitational wave sources in order to improve searches[12,15,16]. In order to quantify the ability of these different models to capture signals from their target sources, we perform effectualness studies. Effectualness is the ability of the waveform template bank to capture the maximal SNR of an ensemble of simulated signals, and is useful for comparing it alongside existing waveform models. It is determined within template bank simulations by calculating the overlap between a template and a signal and maximizing it over both intrinsic and extrinsic parameters. In these simulations, we do not treat the data including noise; however, the power spectral density —which describes how the background is distributed over different frequency ranges —does enter in the calculation of the correlation of two signals.

The first step in our template bank simulations is to construct a template bank for a given parameter space using IMRPhenomC as a waveform model. We then perform simulated injections specifying an injection waveform model, and plot the resulting fitting factors between the templates and injections. We began with studying non-spinning vs. spinning waveform models by injecting aligned-spin IMRPhenomC waveforms into an non-spinning IMRPhenomC template bank. We then compared the IMRPhenomB and IMRPhenomC waveform models by injecting aligned-spin IMRPhenomB waveforms into an aligned-spin IMRPhenomC template bank. We then moved on to studying the recovery of aligned-spin IMRPhenomP waveforms, and finally precessing IMRPhenomP waveforms by the same bank. These effectualness studies demonstrate the ability of this bank to recover precessing signals. Eventually we aim to test the ability of this bank to increase sensitivity to precessing signals (compared to a non-spinning bank) by way of a full pipeline search.

D. The GSTLAL Pipeline

In future work, we plan to implement these methods in a gravitational wave search pipeline. Analysis pipelines identify gravitational wave candidates from multi-detector data. Template bank construction serves as only a small part of the overall pipeline search. GSTLAL is unique from previous pipelines in many ways.[20] It utilizes GStreamer to split the data into separate but synchronized parallel streams, and makes use of multi-banding of the signal.[9] First, a template bank is constructed and the templates undergo time slicing. The bank undergoes a singular value decomposition (SVD), in order to reduce it to fewer waveforms without sacrificing coverage of the parameter space. The data are read into memory and simulated signal injections are made, which are then both whitened following the calculation of a power spectral density (PSD). This whitened data are filtered through all the templates in the bank. At the same time, an auto-correlation chi-squared statistic (defined in Section **??**) is computed. We generate a suite of summary plots which indicate missed and found signals, as well as the sensitivity of the pipeline itself, given by the range, or mean sensitive distance, of the multi-detector network.

In the pipeline, events are ranked according to likelihood[22]. The detection statistic used can be described as a false alarm number of the form

$$x = RT, \tag{14}$$

where R is the false alarm rate (FAR) and T is the duration of the search[9].

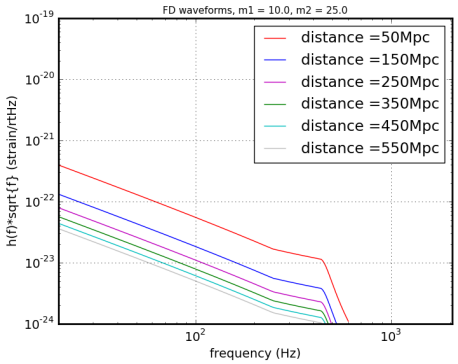

(a)

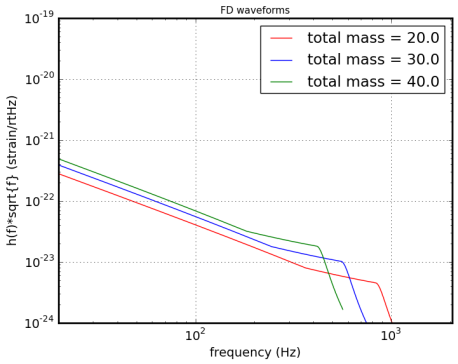

(b)

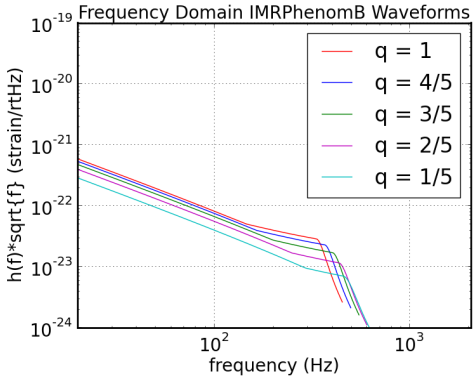

(c)

FIG. 3. a) An example illustrating the dependence of gravitational wave strain on distance from the source. The further the source, the weaker the gravitational wave strain due to energy conservation. b) An example illustrating the dependence of gravitational wave strain on total mass. c) An example illustrating the dependence of gravitational wave strain on mass ratio ($q = \frac{m_1}{m_2}$).

The autocorrelation chi-squared statistic used to distinguish signal from noise is defined as

$$\chi^2 = \int_0^{T_{max}} |\rho(\tau) - \rho_{max}\langle h, he^{2\pi i f\tau}\rangle|^2 \, \mathrm{d}\tau \qquad (15)$$

where T_{max} depends on the degrees of freedom, h represents the signal, ρ_{max} is the SNR maximized over time, and τ is the difference between t_{coal} (See Table I) and the time translation of the template.[9] Large values of χ^2 are deemed glitches and discarded.

IV. RESULTS

A. Template Bank Effectualness

In this work we studied the ability of aligned-spin template banks to capture aligned-spin and precessing spin gravitational wave signals. We studied the template waveforms of the IMRPhenomB and IMRPhenomC models in the spinning and non-spinning cases, and the injection waveforms of generic precessing signals as modeled by IMRPhenomP.

First we tested the ability of a non-spinning IMRPhenomC template bank to recover aligned-spin IMRPhenomC injections (Figure 6), using the parameters from the table in Figure 4. We conclude that a non-spinning IMRPhenomC template bank is effectual at recovering aligned-spin IMRPhenomC injections, even with non-zero aligned spin, everywhere but the high-mass/low-spin and high-spin/low-mass regions.

We then injected aligned-spin IMRPhenomB signals into an IMRPhenomC aligned-spin template bank with the same parameters (from the table in Figure 4). IMRPhenomC performs well recovering aligned-spin signals (even highly-spinning ones) so long as the aligned spin parameter is small; the mean fitting factor falls off rapidly as $|\chi_{eff}| \to 1$ (Figure 7). Despite this, the template bank covers signals with fitting factors greater than 0.97 over most of the parameter space. This supports replacing IMRPhenomB with IMRPhenomC as an IMR waveform model.

After validating the use of the IMRPhenomC model to construct template banks, we moved onto assessing IMRPhenomP as an accurate injection model. We first tested the IMRPhenomP model against the IMRPhenomC model by plotting the waveforms in the frequency domain and then computing the faithfulness of the two. Faithfulness is the degree of overlap (defined in Equation 5) between each waveform with the same intrinsic parameters in two unique waveform models, maximized over all extrinsic parameters. In doing so, we saw no drastic differences in the waveforms.

We then performed effectualness studies on an aligned-spin IMRPhenomC template bank using IMRPhenomC injections as the standard, then aligned-spin IMRPhenomP injections to compare with these, as a test of IMRPhenomP. Finally we injected precessing IMRPhenomP signals into the same bank. We show plots of the fitting factor vs. the injected and best-matched template effective spin parameter χ_{eff} for each of these simulated simulated injections in Figure 8. Figures 8.a, b, and c show aligned-spin IMRPhenomC, aligned-spin IMRPhe-

nomP and precessing-spin IMRPhenomP injections, respectively; in all cases, we use the aligned-spin IMRPhenomC template bank with parameters from the table in Figure 5.

In Figure 9, we plot the fitting factor vs. injected effective spin and effective precessing-spin parameter for precessing IMRPhenomP injections and an aligned-spin IMRPhenomC template bank. This shows that an aligned-spin IMRPhenomC bank is capable of capturing precessing-spin signals for all but the high-spin regions ($\chi_{eff} > 0.5$). This also shows that the IMRPhenomP waveform model behaves as we expect it to in template bank simulations, and is therefore ready to be tested in a full pipeline search.

minimum total mass	10 $M_\odot$
maximum total mass	35 $M_\odot$
maximum mass ratio	4
noise curve	iLIGOSRD
template low frequency cutoff	40 Hz
minimum injected spin	-0.5
maximum injected spin	0.85

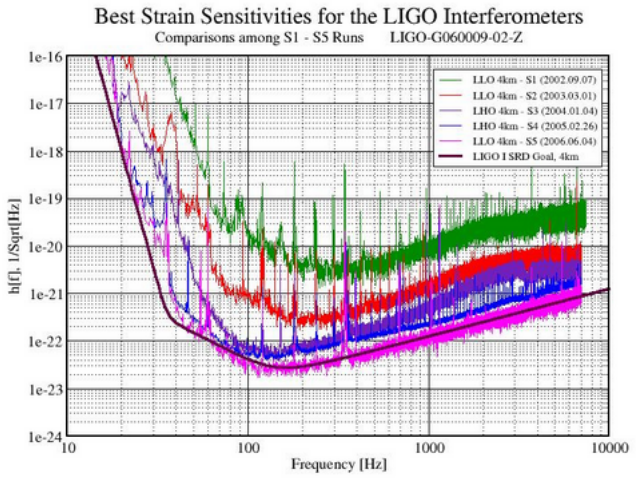

FIG. 4. Above: Parameters used for bank simulation (aligned-spin IMRPhenomC template bank with IMRPhenomB injections). Below: iLIGOSRD stands for Initial LIGO noise amplitude spectral density defined in the LIGO Science Requirements Document[23].

minimum total mass	9.5 $M_\odot$
maximum total mass	50 $M_\odot$
maximum mass ratio	4
template waveform approximant	IMRPhenomC (no spin)
injection waveform approximate	IMRPhenomB (no spin)

TABLE II. Parameters used for preliminary search results using the GSTLAL_inspiral pipeline.

minimum total mass	10 $M_\odot$
maximum total mass	100 $M_\odot$
maximum mass ratio	4
noise curve	aLIGOZeroDetHighPower
template low frequency cutoff	40 Hz
minimum spin	-0.9
maximum spin	0.9

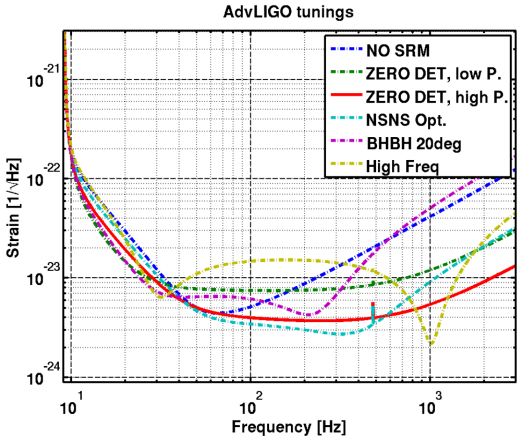

FIG. 5. Above: Parameters used for bank simulations (IMRPhenomC template bank with IMRPhenomC and IMRPhenomP injections). Below: aLIGOZeroDetHighPower stands for Advanced LIGO Zero Detuned High Power, the noise amplitude spectral density (red curve) defined in the LIGO Science Requirements Document, which is very close to what was achieved in LIGO's fifth science run (S5, 2005-2006)[24].

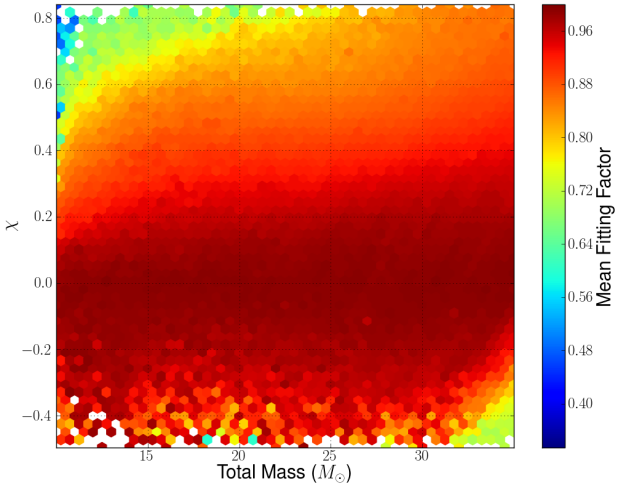

FIG. 6. The mean fitting factor vs. aligned-spin χ_{eff} and injected total mass of the black hole binary for IMRPhenomC waveforms injected into a non-spinning IMRPhenomC template bank. We observe lower recovered SNR for high-mass/low-spin ($M > 31M_\odot$ and $\chi_{eff} < -0.3$) and high-spin/low-mass ($\chi_{eff} > 0.4$ and $M < 20M_\odot$) regions.

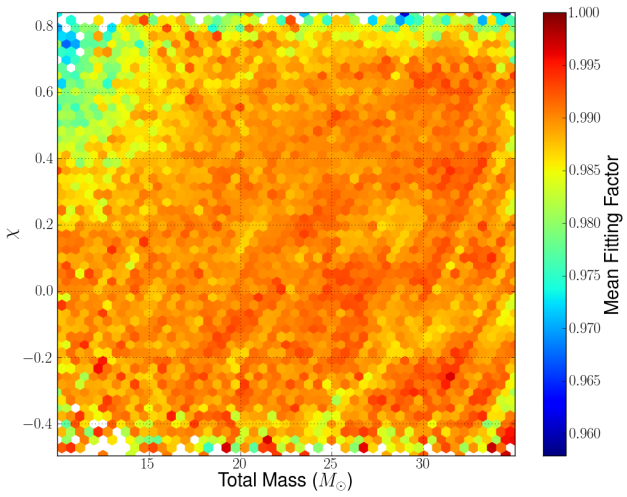

FIG. 7. The mean fitting factor vs. aligned-spin χ_{eff} and injected total mass of the black hole binary for IMRPhenomB waveforms injected into an aligned-spin IMRPhenomC template bank. Note the change in color scale from Figure 6; the mean fitting factor is much closer to 1 over the entire parameter space. We find that matches between the template bank and the injections remain above the $\mathcal{M} = 0.97$ threshold except in very high spin regions of the parameter space ($\chi_{eff} > 0.4$).

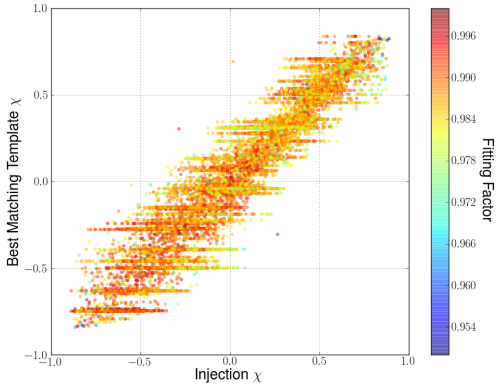

(a)Aligned IMRPhenomC Injections

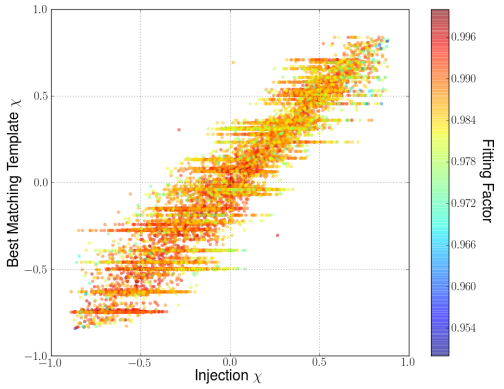

(b)Aligned IMRPhenomP Injections

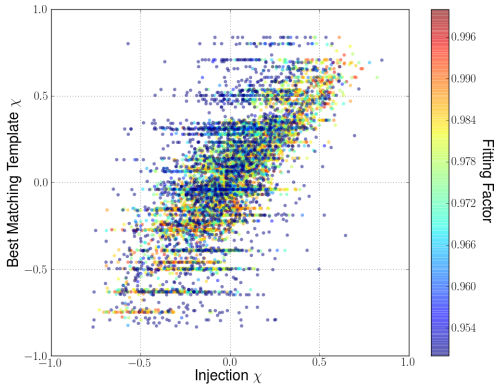

(c)Precessing IMRPhenomP Injections

FIG. 8. Fitting factor vs. injected effective spin parameters and template effective spin parameters for an aligned-spin IMRPhenomC template bank and: a) aligned-spin IMRPhenomC injections, which we expect and see to be fully recovered by the bank, b) aligned-spin IMRPhenomP injections, which we expect and see to be mostly recovered by the bank, since recovery is limited by the slight differences between the two waveform models, and c) precessing spin IMRPhenomP injections, which we do not expect to be fully recovered by an aligned-spin bank. Note that the color scale for the mean fitting factor is the same in a three plots.

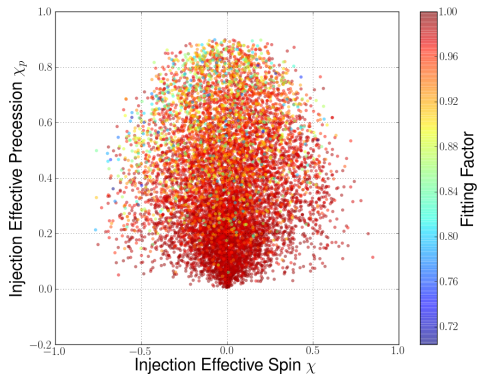

FIG. 9. Fitting factor vs. injected effective precession and injected effective spin parameters for an aligned-spin IMRPhenomC template bank and precessing spin IMRPhenomP injections, which we do not expect to be fully recovered by an aligned-spin bank except at $\chi_p = 0$. We see that as the effective precession increases, the number of matches with $\mathcal{M} > 0.97$ decreases.

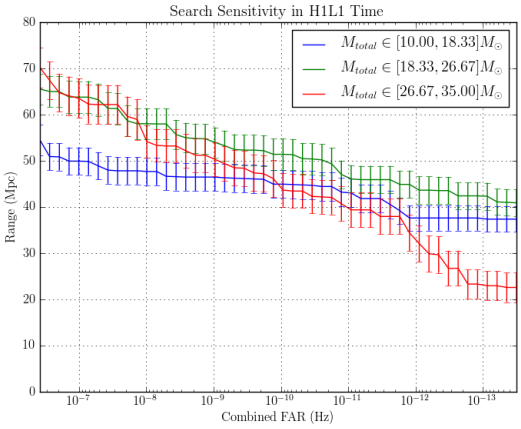

FIG. 10. The sensitive range (in Mpc) of the Initial LIGO detector network to BBHs with total masses in the ranges listed in the legend, as a function of combined False Alarm Rate (see Section **??**. This search was carried out using the `GSTLAL_`inspiral pipeline with a template bank with the parameters in Table II. The sensitive range is comparable to older runs with the same data set, except for the high mass bins, where the range is lower than expected. The relevant FARs for first detection are on the order of 10^{-10} Hz, which corresponds to one false alarm per 30 years.

V. DISCUSSION

We determine that a non-spinning IMRPhenomC template bank recovers aligned-spin IMRPhenomC signals everywhere in the parameter space except for in the high-mass/low-spin ($M > 31M_{\odot}$ and $\chi_{eff} < -0.3$) and high-spin/low-mass ($\chi_{eff} > 0.4$ and $M < 20M_{\odot}$) regions (See Figure 6). This evidence motivates us to move to using an aligned-spin template bank, although this may come with a slight loss in sensitivity (see discussion below) due to increased background associated with a higher number of templates. The move toward inclusion of spinning as well as non-spinnning BBHs, accompanied by increasingly accurate waveform modeling, may well prove to be worth this loss, given its inclusion of a wider range of possible sources. We also see that an aligned-spin IMRPhenomC template bank recovers aligned-spin IMRPhenomB injections everywhere that IMRPhenomB is expected to be valid[15]. This shows that we can move toward using IMRPhenomC as the primary aligned-spin waveform model for the construction of template banks.

We show that IMRPhenomP behaves as expected when injected into an aligned-spin template bank. As the effective precession parameter nears zero, we see that the fitting factor improves, although the fitting factor only drops to around 0.7 for values of χ_p greater than 0.2. This motivates us to accept this model as an injection approximate, although we find small discrepancies related to the way the effective precession parameter is calculated. We believe that conditioning the IMRPhenomC waveforms in the same way as IMRPhenomB will be the next step in using an aligned-spin bank to capture precessing signals in the pipeline. Conditioning consists of the steps taken in the search pipeline (described below) before a waveform is ready to enter the injection stage, including downsampling, normalization, and whitening. We hope to compare the performance of a non-spinning template bank to an aligned-spin bank in order to motivate including spinning templates in the first observation run of Advanced LIGO.

Template bank construction is only a small part of the detection pipeline. The search incorporates data including non-stationary, non-Gaussian detector noise, so that we can more realistically test the detector network. The search separates true detections from false candidate detection events (or glitches), and evaluates the sensitivity of the pipeline in the presence of detector noise. It is expected that including spin effects will improve sensitivity such that the detection rate of gravitational waves is noticeably increased. This will serve to improve searches for compact binary coalescence in Advanced LIGO data. These techniques will allow for greater detection rates and provide more information about the CBC sources in future work.

Upcoming goals include fully implementing the IMRPhenomP model in the existing pipeline search. Problems with the `GSTLAL` code have impeded progress on our goal of using an IMRPhenomC aligned spin template bank, as well as an IMRPhenomB non-spinning template bank, to characterize how well they capture IMRPhenomP injected signals relative to one another. Following a run with IMRPhenomB injections against a non-spinning IMRPhenomC template bank, we discovered that IMRPhenomC waveforms were not being conditioned as they should be. The range of the Hanford and Livingston detectors is plotted in Figure 10, which shows that our sensitivity is lacking for sources with high total mass. Range is the distance out to which the search identifies an injection above the given FAR.

Future work includes transforming the IMRPhenomP waveforms into the time domain to eventually use them as injections in the full search pipeline. After pipeline runs with recolored Advanced LIGO background noise, we hope to find that the recovery of simulated precessing signals from the pipeline is increased with aligned spin templates.

ACKNOWLEDGMENTS

I would like to thank Stephen Privitera, Alan Weinstein, Tjonnie Li, and the rest of the CBC BBH group for their guidance, support, and feedback throughout this project. I gratefully acknowledge the National Science Foundation and the National Society of Hispanic Physicists for funding this work.

[1] Hartle, James B. Gravity: An introduction to Einstein's general relativity. Vol. 1. 2003.

[2] Weisberg, Joel M., and Joseph H. Taylor. "The relativistic binary pulsar b1913+ 16: Thirty years of observations and analysis." Binary Radio Pulsars. Vol. 328. 2005.

[3] Kramer, Michael, et al. "Tests of general relativity from timing the double pulsar." Science 314.5796 (2006): 97-102.

[4] Harry, Gregory M., and LIGO Scientific Collaboration. "Advanced LIGO: the next generation of gravitational wave detectors." Classical and Quantum Gravity 27.8 (2010): 084006.

[5] Advanced Virgo Baseline Design, The Virgo Collaboration, note VIR027A09, May 2009, https://tds.ego-gw.it/itf/tds/file.php?callFile=VIR-0027A-09.pdf

[6] Grote, Hartmut, and LIGO Scientific Collaboration. "The status of GEO 600." Classical and Quantum Gravity 25.11 (2008): 114043.

[7] Postnov, Konstantin A., and Lev R. Yungelson. "The evolution of compact binary star systems." Living Rev. Relativity 9.6 (2006).

[8] Hanna, Chad. "Searching for gravitational waves from

binary systems in non-stationary data." Diss. Louisiana State University, 2008.

[9] Privitera, Stephen M. "The importance of spin for observing gravitational waves from coalescing compact binaries with LIGO and Virgo." Diss. California Institute of Technology, 2014.

[10] Privitera, Stephen, et al. "Improving the sensitivity of a search for coalescing binary black holes with nonprecessing spins in gravitational wave data." Physical Review D 89.2 (2014): 024003.

[11] Hannam, Mark, et al. "Twist and shout: A simple model of complete precessing black-hole-binary gravitational waveforms." arXiv preprint arXiv:1308.3271 (2013).

[12] Taracchini, Andrea, et al. "Effective-one-body model for black-hole binaries with generic mass ratios and spins." Physical Review D 89.6 (2014): 061502.

[13] Sathyaprakash, B. S., and Bernard F. Schutz. "Physics, astrophysics and cosmology with gravitational waves." Living Rev. Relativity 12.2 (2009).

[14] Ajith, Parameswaran, et al. "Template bank for gravitational waveforms from coalescing binary black holes: Nonspinning binaries." Physical Review D 77.10 (2008): 104017.

[15] Ajith, P., et al. "Inspiral-merger-ringdown waveforms for black-hole binaries with nonprecessing spins." Physical review letters 106.24 (2011): 241101.

[16] Santamaria, L., et al. "Matching post-Newtonian and numerical relativity waveforms: Systematic errors and a new phenomenological model for nonprecessing black hole binaries." Physical Review D 82.6 (2010): 064016.

[17] Pan, Yi, et al. "Inspiral-merger-ringdown multipolar waveforms of nonspinning black-hole binaries using the effective-one-body formalism." Physical Review D 84.12 (2011): 124052.

[18] Buonanno, Alessandra, et al. "Approaching faithful templates for nonspinning binary black holes using the effective-one-body approach." Physical Review D 76.10 (2007): 104049.

[19] Taracchini, Andrea, et al. "Prototype effective-one-body model for nonprecessing spinning inspiral-merger-ringdown waveforms." Physical Review D 86.2 (2012): 024011.

[20] Babak, S., et al. "Searching for gravitational waves from binary coalescence." Physical Review D 87.2 (2013): 024033.

[21] Ciufolini, Ignazio, et al., eds. Gravitational waves. CRC Press, 2010.

[22] Cannon, Kipp, Chad Hanna, and Drew Keppel. "Method to estimate the significance of coincident gravitational-wave observations from compact binary coalescence." Physical Review D 88.2 (2013): 024025.

[23] Lazzarini, A., and R. Weiss. "LIGO Science Requirements Document (SRD)." internal LIGO document E950018-02-E (1995).

[24] Shoemaker, David. "Advanced LIGO anticipated sensitivity curves." LIGO Document (2010).

[25] Buonanno, Alessandra, et al. "Comparison of post-Newtonian templates for compact binary inspiral signals in gravitational-wave detectors." Physical Review D 80.8 (2009): 084043.

[26] Allen, Bruce. "A chi-squared time-frequency discriminator for gravitational wave detection." Phys. Rev. D, 71:062001, 2005

[27] Allen, Bruce, et al. "FINDCHIRP: an algorithm for detection of gravitational waves from inspiraling compact binaries." Physical Review D 85.12 (2012): 122006.

[28] Creighton, Jolien DE, and Warren G. Anderson. "Gravitational-Wave Physics and Astronomy: An Introduction to Theory, Experiment and Data Analysis." John Wiley & Sons, 2012.

[29] Biswas, Rahul, et al. "Likelihood-ratio ranking of gravitational-wave candidates in a non-Gaussian background." Physical Review D 85.12 (2012): 122008.

[30] Camp, Jordan B., and Neil J. Cornish. "The Status of Gravitational Wave Astronomy." for LIGO Scientific Collaboration: 2-12.

[31] Frei, Melissa. "Comparative Efficiency and Parameter Recovery of Spin Aligned Templates for Compact Binary Coalescence Detection." Diss. The University of Texas at Austin, 2011.

[32] Baird, Emily, et al. "Degeneracy between mass and spin in black-hole-binary waveforms." Physical Review D 87.2 (2013): 024035.